Institute for Software Integrated Systems
Vanderbilt University
Nashville, Tennessee, 37235

Multi-Rate Networked Control of Conic Systems

Nicholas Kottenstette, Heath LeBlanc, Emeka Eyisi, Xenofon Koutsoukos

TECHNICAL REPORT

ISIS-09-108

Abstract— **Implementation uncertainties such as time-varying delay and data loss and having to typically implement a discrete-time-controller can cause significant problems in the design of networked control systems. This paper describes a novel multi-rate digital-control system which preserves stability and provides robustness to such implementation uncertainties. We present necessary conditions for stability of conic systems interconnected over digital-control-networks which can tolerate networked delays and data-loss. We also compare the performance using simulation results of the proposed architecture to that of a classic-digital-control-implementation applied to controlling position of a single-degree of freedom robotic manipulator.**

I. INTRODUCTION

Our team has investigated the use of passivity for the design of Networked Control Systems (NCS) [1] in the presences of time-varying delays [2], [3]. This paper presents an important new step in the design of networked control systems as it applies to control of a conic-(dissipative) plant inside the sector $[a, b]$ in which $-\infty < a < b$, $0 < b \leq \infty$. Passive systems [4] are a special case of conic-(dissipative) systems inside the sector $[0, \infty]$, thus this paper expands the applicability of our framework.

Our approach employs wave variables to transmit information over the network for the feedback control while remaining passive when subject to arbitrary fixed time delays and data dropouts [5], [6]. The primary advantage of using wave variables is that they tolerate most time-varying delays, such as those occurred when using the TCP/IP transmission protocol. In addition, our architecture adopts a multi-rate digital control scheme to account for: i) different time scales at different part of the network; and ii) bandwidth constraints.

This paper provides sufficient conditions for stability of conic systems to be interconnected over wireless networks which can tolerate networked delays, and data-loss. The continuous-time bounded results can be achieved for linear and nonlinear conic systems. The paper also demonstrates how the proposed architecture can be implemented using a new linear passive-sampler. Finally, our architecture can be used to isolate wide-band and correlated noise without affecting stability through the use of a discrete-time anti-aliasing-filter $H_{LP}(z)$ which was synthesized by applying the conic-preserving-*IPESH*-Transform to a high-order Butterworth filter $H_{LP}(s)$.

Section II describes our new high-performance digital control system and provides the analysis and stability results. Section III validates our results by applying our architecture to control the position of a simulated single-degree of freedom haptic paddle. Section IV provides the conclusions of our paper.

II. HIGH PERFORMANCE DIGITAL CONTROL NETWORKS

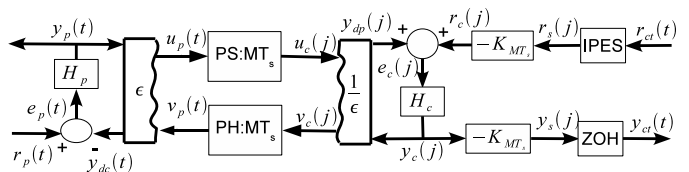Fig. 1 depicts a multi-rate digital control network which interfaces a conic-digital-controller $H_c : e_c \to y_c$ to a

Fig. 1. High Performance, multi-rate digital control network for continuous-time systems.

continuous-time conic plant $H_p : e_p \to y_p$ [7]–[9]. The digital control network is a hybrid-network consisting of both continuous-time wave variables $(u_p(t), v_p(t))$ and discrete-time wave variables $(u_c(j), v_c(j))$ in which $j = \lfloor \frac{t}{MT_s} \rfloor$ [5], [6], [10]. The relationships between the continuous-time and discrete-time wave variables is determined by the multi-rate-passive-sampler (denoted PS : MT_s) and multi-rate-passive-hold (denoted PH : MT_s). These two elements are combination of the passive-sampler and passive-hold blocks (which have been instrumental in showing how to interconnect digital-controllers to continuous-time systems in order to achieve L_2^m-stability [2], [10] see [11], [12] for interconnecting continuous time-plants to continuous-time-controllers over digital networks) and a discrete-time passive-up-sampler and passive-down-sampler [3]. At the interface to the digital controller is an inner-product-equivalent sample and zero-order hold block $y_{ct}(t) = y_s(j)$, $t \in [jMT_s, (j + 1)MT_s)$ [10] which are used *for analysis* in order to relate continuous-time-control-inputs $r_{ct}(t)$ and continuous-time-control-outputs $y_{ct}(t)$ to the continuous-time-plant inputs $r_p(t)$ and outputs $y_p(t)$.

The architecture has the following advantages over traditional digital control systems: 1) L_2^m-stability can be guaranteed for all (non)-linear (dissipative)-conic plants H_p inside the sector $[a_p, b_p]$ in which $-\infty < a_p < b_p$, $0 \leq b_p \leq \infty$, $|a_p| < b_p$; 2) the PS : MT_s can be implemented as a high-order anti-aliasing filter in order to more effectively remove wide-band, and correlated noise introduced into the signal $y_p(t)$ without adversely affecting stability.

By choosing, to use wave-variables, a negative output feedback loop is introduced for both the plant and controller in which we provide the analysis to determine its effects in Section II-A. This analysis in which we consider boundedness results for *digital control* is inspired by the insightful *continuous-time control* results presented in [13] in which the plant-disturbance *was not considered* ($r_p(t) = 0$). Section II-B introduces the multi-rate-passive-sampler and multi-rate-passive-hold which includes a *new linear* passive-sampler which will encourage further analysis and simplify implementation, it also includes our main stability results. Section II-C provides the necessary results to construct conic-digital-filters (which are inside the sector $[a_f, b_f]$ from conic-continuous-time-filters which are inside the sector $[a_f, b_f]$.

A. Control of Conic-Dissipative Systems

In order to leverage the pioneering work of [7], [8] in regards to the control of conic-systems and connect it to

dissipative systems theory [14]. We shall consider the following class of causal non-linear finite-dimensional continuous-time (discrete-time) systems $H : u \to y$ which are affine in control:

$$\dot{x}(t) = f(x(t)) + G(x(t))u(t), \ x(0) = x_0 = 0, \ t \geq 0 \quad (1)$$
$$y(t) = h(x(t)) + J(x(t))u(t)$$

for the continuous-time case in which the functions indicated in (1) are sufficiently smooth to make the system well defined [15], and

$$x(j+1) = f(x(j)) + G(x(j))u(j), \ x(0) = x_0 = 0 \quad (2)$$
$$y(j) = h(x(j)) + J(x(j))u(j)$$

for the discrete time case $(j = \{0, 1, \dots\})$ in which $x \in \mathbb{R}^n$, $u, y \in \mathbb{R}^m$ in which n and m are positive integers. In addition it is assumed that there exists a finite-square-integrable (summable) function $u()$ such that all $x \in \mathbb{R}^n$ are reachable from the zero-state x_0. Finally it is assumed that x_0 is the only equilibrium point such that $f(x_0) = 0$ and $f(x) \neq 0$ when $x \neq x_0$. Finally, we shall consider the following interior conic-dissipative supply function $s(u, y)$ as it relates to conic-dissipative systems which are inside the sector $[a, b]$ $(a < b)$ [16]–[18]:

$$s(u, y) = \begin{cases} -y^{\mathsf{T}}y + (a+b)y^{\mathsf{T}}u - abu^{\mathsf{T}}u, & |a|, |b| < \infty \\ y^{\mathsf{T}}u - au^{\mathsf{T}}u, & |a| < \infty, \ b = \infty. \end{cases} \quad (3)$$

Definition 1: The continuous-time system $H : u \to y$, $x_0 = x(0) = 0$ whose dynamics are determined by (1) is a continuous-conic-dissipative system inside the sector $[a, b]$ with respect to the supply (3) if:

$$\int_0^T s(u, y)dt \geq 0, \ T \in \mathbb{R} \geq 0. \quad (4)$$

Analogously the discrete-time system $H : u \to y$, $x_0 = x(0) = 0$ whose dynamics are determined by (2) is a discrete-conic-dissipative system inside the sector $[a, b]$ with respect to the supply (3) if:

$$\sum_{j=0}^{N-1} s(u, y) \geq 0, \ \forall N \in \{1, 2, \dots\}. \quad (5)$$

NB. the smoothness condition required by [15] appears to limit the discussion to systems which have finite-state-space descriptions and the resulting control system we will examine will be subject to time-delays which result in an infinite state-space. Therefore, if functions indicated in (1) are *not* sufficiently smooth but (4) is satisfied then the system $H : u \to y$ is a *continuous-conic system* inside the sector $[a, b]$. Finally the following notation will be used in order to represent time integrals, sums and norms:

$$\langle y, u \rangle_T = \int_0^T y^{\mathsf{T}}(t)u(t)dt; \quad \|(y)_T\|_2^2 = \langle y, y \rangle_T$$
$$\langle y, u \rangle_N = \sum_{j=0}^{N-1} y^{\mathsf{T}}(j)u(j); \quad \|(y)_N\|_2^2 = \langle y, y \rangle_N$$
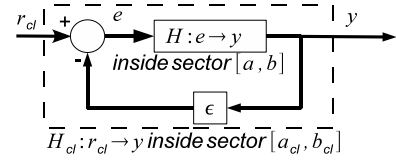$$\|y(t)\|_2^2 = \lim_{T \to \infty} \|(y)_T\|_2^2; \quad \|y(j)\|_2^2 = \lim_{N \to \infty} \|(y)_N\|_2^2.$$

Fig. 2. Nominal closed-loop system H_{cl} resulting from ϵ and H_s.

If it is clear that y is either a continuous or discrete-time function then the two-norm of y will be denoted simply $\|y\|_2$.

From [15], [18] in regards to Lyapunov stability and from [7]–[9] in regards to L_2^m (l_2^m) stability conic-dissipative systems have the following important properties:

Property 1: There exists a storage function $V(x) \geq 0$ $\forall x \neq 0$, $V(0) = 0$ such that: i) $\dot{V}(x) \leq s(u, y)$ for a continuous-conic-dissipative system; and
ii) $V(x(j+1)) - V(x(j)) \leq s(u(j), y(j))$ for a discrete-time-conic-dissipative system. If in addition $h(x_0) = J(x)0 = 0$ and $h(x) \neq 0$ when $x \neq 0$ so that $H : u \to y$ is zero-state detectable then $V(x) > 0$ $\forall x \neq 0$. Therefore if $H : u \to y$ is inside the sector $[a, b]$:

i) and zero-state detectable and $|a| < \infty$, $b = \infty$ it is Lyapunov stable.

ii) and zero-state detectable and $|a|, |b| < \infty$ it is asymptotically stable.

iii) and $|a|, |b| < \infty$ then it is inside the sector $[-\gamma, \gamma]$ in which $\gamma = \max\{|a|, |b|\}$. Therefore, it is $L_2^m(l_2^m)$-stable in which:

$$\|y\|_2 \leq \gamma \|u\|_2. \quad (6)$$

iv) and $k \geq 0$ then kH is inside the sector $[ka, kb]$; $-kH$ is inside the sector $[-kb, -ka]$.

v) (Sum Rule) if in addition $H_1 : u_1 \to y_1$ is inside the sector $[a_1, b_1]$ then $(H + H_1) : u \to (y + y_1)$ is inside the sector $[a + a_1, b + b_1]$.

We are particularly interested in determining the resulting gain $g(H_{\text{cl}})$ $(\|(y_s)_T\|_2 \leq g(H_{\text{cl}})\|(r_{\text{cl}})_T\|_2)$ when closing the loop of a conic-system H_s which is inside the sector $[a_s, b_s]$ as depicted in Fig. 2.

Theorem 1: The conic-system $H : e \to y$ depicted in Fig. 2 is inside the sector $[a, b]$, $\epsilon > 0$. The input e is related to the reference r_{cl} and output y by the following feedback equation: $e(t) = r_{\text{cl}}(t) - \epsilon y(t)$, $\forall t \geq 0$. The resulting closed-loop system is denoted $H_{\text{cl}} : r_{\text{cl}} \to y$. For the case when:

I. $0 \leq a < b \leq \infty$, H_{cl} is inside the sector $[\frac{a}{1+\epsilon a}, \frac{b}{1+\epsilon b}]$ in which $g(H_{\text{cl}}) = \frac{b}{1+\epsilon b}$.

II. $a < 0$, $-a < b \leq \infty$, $0 \leq \epsilon < -\frac{1}{2}\left(\frac{1}{a} + \frac{1}{b}\right)$ then H_{cl} is inside the sector $[\frac{a}{1+\epsilon a}, \frac{b}{1+\epsilon b}]$ in which $g(H_{\text{cl}}) = \frac{b}{1+\epsilon b}$.

Proof:

I. If $(a+b) > 0$ then our conic-system $H : e \to y$ satisfies

$$\langle y, e \rangle_T \geq \frac{1}{a+b}\|(y)_T\|_2^2 + \frac{ab}{a+b}\|(e)_T\|_2^2.$$

Substituting in the feedback equation for e results in

$$\langle y, r_{\text{cl}} \rangle_T \geq \left(\epsilon + \frac{1}{a+b}\right)\|(y)_T\|_2^2 +$$
$$\frac{ab}{a+b}\|(r_{\text{cl}} - \epsilon y)_T\|_2^2.$$

Denote $c_1 = \dfrac{a + b + 2\epsilon ab}{a + b}$.

Solving for the norm of the feedback-error results in

$$c_1 \langle y, r_{\mathsf{cl}} \rangle_T \geq \frac{1 + \epsilon(a + b) + \epsilon^2 ab}{a + b} \|(y)_T\|_2^2 +$$
$$\frac{ab}{a + b} \|(r_{\mathsf{cl}})_T\|_2^2.$$

Dividing both sides by c_1 results in

$$\langle y, r_{\mathsf{cl}} \rangle_T \geq \frac{1}{a_{\mathsf{cl}} + b_{\mathsf{cl}}} \|(y)_T\|_2^2 + \frac{a_{\mathsf{cl}} b_{\mathsf{cl}}}{a_{\mathsf{cl}} + b_{\mathsf{cl}}} \|(r_{\mathsf{cl}})_T\|_2^2$$

in which $a_{\mathsf{cl}} = \dfrac{a}{1 + \epsilon a}$, $b_{\mathsf{cl}} = \dfrac{b}{1 + \epsilon b}$.

II. We observe when $a < 0$ and $-a < b \leq \infty$ then if $0 \leq \epsilon < -\frac{1}{2}\left(\frac{1}{a} + \frac{1}{b}\right)$ holds then $c_1 > 0$ therefore all the inequalities for proving the previous case hold.
$g(H_{\mathsf{cl}}) = \frac{b}{1 + \epsilon b}$ is a direct result from Property 1-iii). ∎

1) Wave Variable Networks: In order to analyze the closed-loop effects on H_p and H_c we recall our use of wave-variables. As discussed in [10] scattering [19] or their reformulation known as the wave-variable-networks allow *controller* and *plant* variables $(y_c(j), y_p(t))$, to be transmitted over a network while remaining *passive* when subject to arbitrary fixed time delays and data dropouts [5]. Denote $I \in \mathbb{R}^{m \times m}$ as the identity matrix. When implementing the wave variable transformation the continuous time plant "outputs" $(u_p(t), y_{\mathsf{dc}}(t))$ are related to the corresponding "inputs" $(v_p(t), y_p(t))$ as follows (Fig. 1):

$$\begin{bmatrix} u_p(t) \\ y_{\mathsf{dc}}(t) \end{bmatrix} = \begin{bmatrix} -I & \sqrt{2\epsilon}I \\ -\sqrt{2\epsilon}I & \epsilon I \end{bmatrix} \begin{bmatrix} v_p(t) \\ y_p(t) \end{bmatrix} \quad (7)$$

Next, the discrete time controller "outputs" $(v_c(j), y_{\mathsf{dp}}(j))$ are related to the corresponding "inputs" $(u_c(j), y_c(j))$ as follows (Fig. 1):

$$\begin{bmatrix} v_c(j) \\ y_{\mathsf{dp}}(j) \end{bmatrix} = \begin{bmatrix} I & -\sqrt{\frac{2}{\epsilon}}I \\ \sqrt{\frac{2}{\epsilon}}I & -\frac{1}{\epsilon}I \end{bmatrix} \begin{bmatrix} u_c(j) \\ y_c(j) \end{bmatrix} \quad (8)$$

It has been shown that the digital control network for $M = 1$ depicted in Fig. 1 results in a L_2^m-stable system *if the discrete-time-controller H_c is strictly-output-passive (inside the sector $[0, b_c]$) and the continuous-time plant H_p is strictly-output-passive (inside the sector $[0, b_p]$)* [2], [10]. In order to study the case when H_p is not passive we need to: i) explicitly consider the network structure which results from using wave variables; and ii) use Assumption 1.

Assumption 1: The plant depicted in Fig. 1 H_p is inside the sector $[a_p, b_p]$ in addition the controller H_c is inside the sector $[a_c, b_c]$ ($a_c \geq 0$) in addition the scattering gain ϵ satisfies the following bounds: i) $0 < \epsilon < \infty$, if $a_p \geq 0$; or ii) $0 < \epsilon < -\frac{1}{2}\left(\frac{1}{a_p} + \frac{1}{b_p}\right)$, if $a_p < 0$.
Assumption 1, Lemma 4 and Lemma 5 (see Appendix) allow us to state Theorem 2.

Theorem 2: The plant-controller-network depicted in Fig. 1 can be transformed to the final form depicted in Fig. 3 if Assumption 1 is satisfied. The transformed plant subsystem $\sqrt{2\epsilon}H_{\mathsf{pe}} : \hat{e}_{\mathsf{clp}} \to y_{\mathsf{pe}}$ is denoted with the shorthand notation $\sqrt{2\epsilon}H_{\mathsf{pe}}$ in which: i) $\hat{e}_{\mathsf{clp}}(t) = \frac{1}{\sqrt{2\epsilon}} r_p(t) + v_p(t)$; and
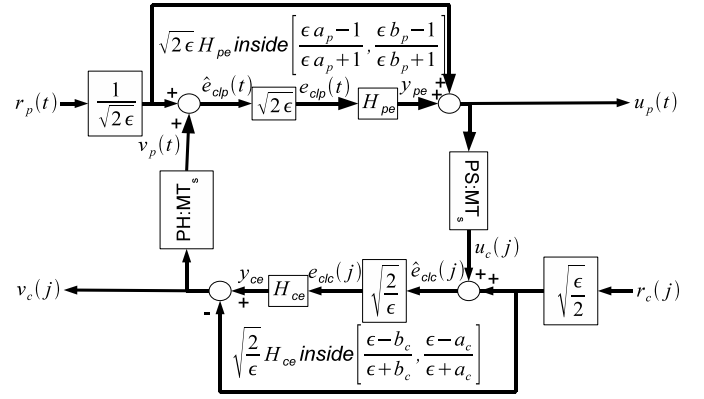

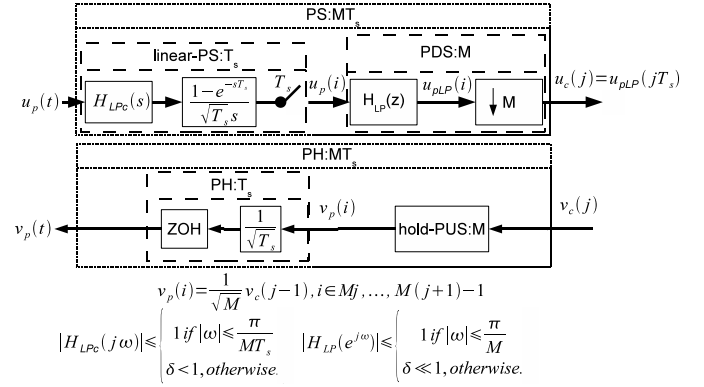Fig. 3. Final Controller-Plant-wave-network realization.

Fig. 4. Multi-rate passive-sampler, passive-hold.

ii) $y_{\mathsf{pe}}(t) = \sqrt{2\epsilon}y_p(t) - \hat{e}_{\mathsf{clp}}(t)$ hold. In addition the transformed control subsystem $\sqrt{\frac{2}{\epsilon}}H_{\mathsf{ce}} : \hat{e}_{\mathsf{clc}} \to y_{\mathsf{ce}}$ is denoted with the shorthand notation $\sqrt{\frac{2}{\epsilon}}H_{\mathsf{ce}}$ in which: i) $\hat{e}_{\mathsf{clc}}(j) = \sqrt{\frac{\epsilon}{2}}r_c(j) + u_c(j)$; and ii) $y_{\mathsf{ce}}(t) = \sqrt{\frac{2}{\epsilon}}y_c(j) + \hat{e}_{\mathsf{clc}}(j)$ hold. Each is a conic-dissipative system such that

$\sqrt{2\epsilon}H_{\mathsf{pe}}$ is inside the sector $\left[\dfrac{\epsilon a_p - 1}{\epsilon a_p + 1}, \dfrac{\epsilon b_p - 1}{\epsilon b_p + 1}\right]$ and

$\sqrt{\dfrac{2}{\epsilon}}H_{\mathsf{ce}}$ is inside the sector $\left[\dfrac{\epsilon - b_c}{\epsilon + b_c}, \dfrac{\epsilon - a_c}{\epsilon + a_c}\right]$.

B. Multi-Rate-Passive-Sampler(Hold)

Fig. 4 depicts our proposed multi-rate passive-sampler (PS:MT_s), and passive-hold (PH:MT_s) subsystem. The multi-rate passive-sampler (PS:MT_s) consists of a cascade of a linear-passive-sampler (linear-PS:T_s) and a passive-downsampler (PDS:M). The multi-rate passive-hold (PH:MT_s) subsystem consists of a cascade of a hold-passive-upsampler (hold-PUS:M) and passive-hold (PH:T_s). For simplicity of discussion the figure is for the single-input-single-output (SISO) case but we note all elements depicted can be diagonalized to handle m-dimensional waves. The standard anti-aliasing down-sampler $(H_{LP}(z), \downarrow M)$ system depicted in Fig. 4 has been shown to be a PDS, in addition the hold-PUS depicted is a PUS [3, Definition 4]. A valid

PDS:M and PUS:M satisfy the following inequalities:

$$\|(u_c(j))_N\|_2^2 \leq \|(u_p(i))_{MN}\|_2^2 \tag{9}$$

$$\|(v_p(i))_{MN}\|_2^2 \leq \|(v_c(j))_N\|_2^2 \tag{10}$$

which hold $\forall N \geq 0$. The scaled-*ZOH* block in which

$$v_p(t) = \frac{1}{T_s} v_p(i), \ t \in [iT_s, (i+1)T_s)$$

has been shown to be a valid passive-hold system PH:T_s in which

$$\|(v_p(t))_{MNT_s}\|_2^2 \leq \|(v_p(i))_{MN}\|_2^2 \tag{11}$$

[2]. A valid passive-sampler will satisfy the following inequality

$$\|(u_p(i))_{MN}\|_2^2 \leq \|(u_p(t))_{MNT_s}\|_2^2, \tag{12}$$

unlike the non-linear averaging-passive-sampler [10, Definition 6] implementation which was shown to be a valid PS we choose to implement a linear version.

Definition 2: The linear-passive-sampler (Fig. 4) with input $u_p(t)$ and output $u_p(i)$ is implemented as follows:

1. $u_p(t)$ passes through an analog low-pass anti-aliasing filter denoted $H_{\mathsf{LPc}}(s)$ whose magnitude $|H_{\mathsf{LPc}}(j\omega)| \leq 1$ with passband $\omega_p = \frac{\pi}{MT_s}$ and stop-band $\omega_s = \frac{\pi}{T_s}$ [20].
2. the output of $H_{\mathsf{LPc}}(s)$ we denote as $u_{pLPc}(t)$ in which

$$u_p(i) = \frac{1}{\sqrt{T_s}} \int_0^{iT_s} (u_{pLPc}(t) - u_{pLPc}(t-T_s))dt \tag{13}$$

Lemma 1: The linear-passive-sampler (Definition 2) satisfies (12).

Proof: Since $u_p(t) = 0$, $t < 0$ by assumption, and the low-pass-filter is assumed to be causal therefore $u_p(0) = 0$ which implies that

$$0 = \|(u_p(i))_0\|_2^2 \leq \|(u_p(t))_0\|_2^2.$$

Next, we note that (13) can be equivalently written as

$$u_p(i) = \frac{1}{\sqrt{T_s}} \int_{(i-1)T_s}^{iT_s} u_{pLPc}(t)dt$$

squaring both sides we have

$$u_p^2(i) = \frac{1}{T_s}(\int_{(i-1)T_s}^{iT_s} u_{pLPc}(t)dt)^2$$

applying the Schwarz Inequality we have

$$u_p^2(i) \leq \frac{T_s}{T_s} \int_{(i-1)T_s}^{iT_s} u_{pLPc}^2(t)dt$$

therefore

$$
\begin{aligned}
\|(u_p(i))_{MN}\|_2^2 &= \sum_{i=0}^{MN-1} u_p^2(i) \\
&\leq \sum_{i=0}^{MN-1} \int_{(i-1)T_s}^{iT_s} u_{pLPc}^2(t)dt \\
&\leq \|(u_{pLPc}(t))_{(MN-1)T_s}\|_2^2 \\
&\leq \|(u_{pLPc}(t))_{MNT_s}\|_2^2
\end{aligned}
$$

since the low-pass-filter has a gain less than or equal to one ($\|(u_{pLPc}(t))_{MNT_s}\|_2^2 \leq \|(u_p(t))_{MNT_s}\|_2^2$) then (12) clearly results from these last two inequalities. ∎

Finally, from (9) and (12) it is obvious that the following inequality holds for the multi-rate-passive-sampler PS:MT_s

$$\|(u_c(j))_N\|_2^2 \leq \|(u_p(t))_{MNT_s}\|_2^2 \tag{14}$$

and from (11) and (10) the following holds for the multi-rate-passive-hold PH:MT_s

$$\|(v_p(t))_{MNT_s}\|_2^2 \leq \|(v_c(j))_N\|_2^2 \tag{15}$$

With these two inequalities established, and Theorem 2 we can now prove the following Lemma.

Lemma 2: Denote the L_2^m-gain of the plant-subsystem $\sqrt{2\epsilon}H_{\mathsf{pe}} : \hat{e}_{\mathsf{clp}} \rightarrow y_{\mathsf{pe}}$ as γ_{pe} in which $\|(y_{\mathsf{pe}})_{MNT_s}\|_2 \leq \gamma_{\mathsf{pe}}\|(\hat{e}_{\mathsf{clp}})_{MNT_s}\|_2$. In addition, denote the l_2^m-gain of the controller-subsystem $\sqrt{\frac{2}{\epsilon}}H_{\mathsf{ce}} : \hat{e}_{\mathsf{clc}} \rightarrow y_{\mathsf{ce}}$ as γ_{ce} in which $\|(y_{\mathsf{ce}})_N\|_2 \leq \gamma_{\mathsf{ce}}\|(\hat{e}_{\mathsf{clc}})_N\|_2$. In addition we shall use the following shorthand notation in which $\hat{E}_{\mathsf{clp}} = \|(\hat{e}_{\mathsf{clp}})_{MNT_s}\|_2$, $\hat{E}_{\mathsf{clc}} = \|(\hat{e}_{\mathsf{clc}})_N\|_2$, $R_p = \|(r_p)_{MNT_s}\|_2$, and $R_c = \|(r_c)_N\|_2$. If $\gamma_{\mathsf{pe}}\gamma_{\mathsf{ce}} < 1$ then

$$\hat{E}_{\mathsf{clc}} \leq \frac{\gamma_{\mathsf{pe}} + 1}{1 - \gamma_{\mathsf{pe}}\gamma_{\mathsf{ce}}} \left(\sqrt{\frac{\epsilon}{2}}R_c + \frac{1}{\sqrt{2\epsilon}}R_p\right)$$

$$\hat{E}_{\mathsf{clp}} \leq \frac{\gamma_{\mathsf{ce}} + 1}{1 - \gamma_{\mathsf{pe}}\gamma_{\mathsf{ce}}} \left(\sqrt{\frac{\epsilon}{2}}R_c + \frac{1}{\sqrt{2\epsilon}}R_p\right)$$

Proof: From the triangle inequality we have:

$$\|(\hat{e}_{\mathsf{clp}})_{MNT_s}\|_2 \leq \frac{1}{\sqrt{2\epsilon}}\|(r_p)_{MNT_s}\|_2 + \|(v_p)_{MNT_s}\|_2 \tag{16}$$

$$\|(\hat{e}_{\mathsf{clc}})_N\|_2 \leq \sqrt{\frac{\epsilon}{2}}\|(r_c)_N\|_2 + \|(u_c)_N\|_2 \tag{17}$$

$$\|(u_c)_N\|_2 \leq \gamma_{\mathsf{pe}}\|(\hat{e}_{\mathsf{clp}})_{MNT_s}\|_2 + \frac{1}{\sqrt{2\epsilon}}\|(r_p)_{MNT_s}\|_2 \tag{18}$$

$$\|(v_p)_{MNT_s}\|_2 \leq \gamma_{\mathsf{ce}}\|(\hat{e}_{\mathsf{clc}})_N\|_2 + \sqrt{\frac{\epsilon}{2}}\|(r_c)_N\|_2 \tag{19}$$

in which the final two inequalities were a direct result of (14) and (15) respectively. and substituting (19) into (16) results in

$$\hat{E}_{\mathsf{clp}} \leq \gamma_{\mathsf{ce}}\hat{E}_{\mathsf{clc}} + \left(\frac{1}{\sqrt{2\epsilon}}R_p + \sqrt{\frac{\epsilon}{2}}R_c\right) \tag{20}$$

similarly substituting (18) into (17) results in

$$\hat{E}_{\mathsf{clc}} \leq \gamma_{\mathsf{pe}}\hat{E}_{\mathsf{clp}} + \left(\frac{1}{\sqrt{2\epsilon}}R_p + \sqrt{\frac{\epsilon}{2}}R_c\right) \tag{21}$$

Substituting (20) into (21) results in the following

$$\hat{E}_{\mathsf{clc}} \leq \gamma_{\mathsf{pe}}\gamma_{\mathsf{ce}}\hat{E}_{\mathsf{clc}} + (\gamma_{\mathsf{pe}} + 1)\left(\frac{1}{\sqrt{2\epsilon}}R_p + \sqrt{\frac{\epsilon}{2}}R_c\right)$$

$$\hat{E}_{\mathsf{clc}} \leq \frac{\gamma_{\mathsf{pe}} + 1}{1 - \gamma_{\mathsf{pe}}\gamma_{\mathsf{ce}}}\left(\frac{1}{\sqrt{2\epsilon}}R_p + \sqrt{\frac{\epsilon}{2}}R_c\right)$$

likewise, substituting (21) into (20) results in the following

$$\hat{E}_{\mathsf{clp}} \leq \gamma_{\mathsf{pe}}\gamma_{\mathsf{ce}}\hat{E}_{\mathsf{clp}} + (\gamma_{\mathsf{ce}} + 1)\left(\frac{1}{\sqrt{2\epsilon}}R_p + \sqrt{\frac{\epsilon}{2}}R_c\right)$$

$$\hat{E}_{\mathsf{clp}} \leq \frac{\gamma_{\mathsf{ce}} + 1}{1 - \gamma_{\mathsf{pe}}\gamma_{\mathsf{ce}}}\left(\frac{1}{\sqrt{2\epsilon}}R_p + \sqrt{\frac{\epsilon}{2}}R_c\right)$$

note that the inequalities only result if $\gamma_{\mathsf{pe}}\gamma_{\mathsf{ce}} < 1$. ∎

Next we note the following observation that $\gamma_{\mathsf{pe}} = g(\sqrt{2\epsilon}H_{\mathsf{pe}}) = g(-\sqrt{2\epsilon}H_{\mathsf{pe}})$ and $\gamma_{\mathsf{ce}} = g(\sqrt{\frac{2}{\epsilon}}H_{\mathsf{ce}}) = g(-\sqrt{\frac{2}{\epsilon}}H_{\mathsf{ce}})$ therefore using Theorem 1, Theorem 2 the following Corollary follows.

Corollary 1:

$$\gamma_{\mathsf{pe}} = g(\sqrt{2\epsilon}H_{\mathsf{pe}}) = \max\left\{\left|\frac{\epsilon a_p - 1}{\epsilon a_p + 1}\right|, \left|\frac{\epsilon b_p - 1}{\epsilon b_p + 1}\right|\right\} \quad (22)$$

$$\gamma_{\mathsf{ce}} = g(\sqrt{\frac{2}{\epsilon}}H_{\mathsf{ce}}) = \max\left\{\left|\frac{\epsilon - b_c}{\epsilon + b_c}\right|, \left|\frac{\epsilon - a_c}{\epsilon + a_c}\right|\right\} \quad (23)$$

Therefore:

1. when the plant is passive ($a_p = 0$, $b_p = \infty$) then $\gamma_{\mathsf{pe}} = 1$ which implies $\gamma_{\mathsf{pe}}\gamma_{\mathsf{ce}} < 1$ if the controller is strictly-input-output-passive $0 < a_c \leq b_c < \infty$ (and vice-versa).
2. when the plant is inside the sector $[a_p, \infty]$ in which $a_p < 0$ then $\gamma_{\mathsf{pe}}\gamma_{\mathsf{ce}} < 1$ if the controller is inside the sector $[a_c, b_c]$ in which $-\epsilon^2 a_p < a_c, b_c < \frac{-1}{a_p}$.

As was shown in [10] the *IPESH* blocks can be used to aid with analysis such that

$$\|(y_c)_N\|_2 = \frac{1}{\sqrt{MT_s}K_{MT_s}}\|(y_{ct})_{MNT_s}\|_2 \quad (24)$$

holds. In addition, the following inequality result from applying the *Schwarz inequality* as demonstrated in [21, proof of Theorem 1-III].

$$\|(r_c)_N\|_2 \leq \sqrt{MT_s}K_{MT_s}\|(r_{ct})_{MNT_s}\|_2 \quad (25)$$

Theorem 3: When $\gamma_{\mathsf{pe}}\gamma_{\mathsf{ce}} < 1$ the digital control network depicted in Fig. 1 is L_2^m-stable in which there exists a $0 < \gamma < \infty$ such that $\|y(t)\|_2 \leq \gamma\|u(t)\|_2$ in which $y^\mathsf{T}(t) = [y_p^\mathsf{T}(t), y_{ct}^\mathsf{T}(t)]$ and $u^\mathsf{T}(t) = [r_p^\mathsf{T}(t), r_{ct}^\mathsf{T}(t)]$.

Proof: (Sketch) From Corollary 4 in the Appendix we have that $H_{\mathsf{clc}} : e_{\mathsf{clc}} \to y_c$ has finite gain $g(H_{\mathsf{clc}}) = \frac{\epsilon b_c}{\epsilon + b_c}$ and $\sqrt{\frac{2}{\epsilon}}\hat{E}_{\mathsf{clc}} = \|(e_{\mathsf{clc}})_N\|_2$, therefore $\|(y_c)_N\|_2 \leq \frac{\epsilon b_c}{\epsilon + b_c}\sqrt{\frac{2}{\epsilon}}\hat{E}_{\mathsf{clc}}$ substituting (24) for the left-hand-side results in $\frac{1}{\sqrt{MT_s}K_{MT_s}}\|(y_{ct})_{MNT_s}\|_2 \leq \frac{\epsilon b_c}{\epsilon + b_c}\sqrt{\frac{2}{\epsilon}}\hat{E}_{\mathsf{clc}}$. Similarly $\|(y_p)_{MNT_s}\|_2 \leq \frac{b_p}{1 + \epsilon b_p}\sqrt{2\epsilon}\hat{E}_{\mathsf{clp}}$ holds since from Corollary 3 in the Appendix we know that the closed-loop plant $H_{\mathsf{clp}} : e_{\mathsf{clp}} \to y_{\mathsf{clp}}$ has finite-gain $g(H_{\mathsf{clp}}) = \frac{b_p}{1 + \epsilon b_p}$ and that $\sqrt{2\epsilon}\hat{E}_{\mathsf{clp}} = \|(e_{\mathsf{clp}})_{MNT_s}\|_2$. Finally, we observe that (25) along with the other continuous-time-norm inequalities can be substituted into the final-two inequalities of Lemma 2 such that both inequalities involve only continuous-time norms in which the outputs $y_p(t)$ and $y_{ct}(t)$ are bounded by the inputs $r_p(t)$ and $r_{ct}(t)$. Therefore, when $\gamma_{\mathsf{pe}}\gamma_{\mathsf{ce}} < 1$ the digital control network depicted in Fig. 1 is L_2^m-stable. ∎

C. Conic Digital Filters

The section shows how an engineer can synthesize a discrete-time controller/filter from a continuous-time reference model. In particular, we show how a continuous-time conic system can be transformed into a discrete-time conic system using the *inner-product equivalent sample and hold*

(IPESH). Additionally, we present a corollary for transforming a continuous-time conic single-input-single-output (SISO) linear time-invariant *(LTI)* system into a discrete-time conic SISO *LTI* system using the *IPESH*-Transform. We begin by recalling the definition for the *IPESH* which is based on the earlier work of [22], [23].

Definition 3: [24, Definition 4] Let a continuous one-port plant be denoted by the input-output mapping $H_{ct} : L_{2_e}^m \to L_{2_e}^m$. Denote continuous time as t, the discrete time index as i, the sample and hold time as T_s, the continuous input as $u(t) \in L_{2_e}^m$, the continuous output as $y(t) \in L_{2_e}^m$, the transformed discrete input as $u(i) \in l_{2_e}^m$, and the transformed discrete output as $y(i) \in l_{2_e}^m$. The *inner-product equivalent sample and hold* (IPESH) is implemented as follows:

I. $x(t) = \int_0^t y(\tau)d\tau$
II. $y(i) = x((i+1)T_s) - x(iT_s)$
III. $u(t) = u(i), \forall t \in [iT_s, (i+1)T_s)$

As a result $\langle y(i), u(i)\rangle_N = \langle y(t), u(t)\rangle_{NT_s}$ holds $\forall N \geq 1$.

Lemma 3: If H_{ct} is inside the sector $[a, b]$ then H_d resulting from the *IPESH* is inside the sector $[aT_s, bT_s]$.

Proof: Since H_{ct} is inside the sector $[a, b]$, we can write

$$\langle y, u\rangle_T \geq \frac{1}{a + b}\|(y)_T\|_2^2 + \frac{ab}{a + b}\|(u)_T\|_2^2. \quad (26)$$

But, from Definition 3-III it can be shown that

$$\|(u)_T\|_2^2 = T_s\|(u)_N\|_2^2. \quad (27)$$

Additionally, from Definition 3-II and the *Schwarz inequality*, the following inequality can be shown to hold [21, proof of Theorem 1-III]

$$\|(y)_T\|_2^2 \geq \frac{1}{T_s}\|(y)_N\|_2^2. \quad (28)$$

Finally, we use the equivalence of the discrete-time and continuous-time inner products combined with (27) and (28), and substitute into (26) to obtain

$$\langle y, u\rangle_N \geq \frac{1}{T_s(a+b)}\|(y)_N\|_2^2 + \frac{abT_s}{a + b}\|(u)_N\|_2^2$$
$$= \frac{1}{(aT_s) + (bT_s)}\|(y)_N\|_2^2 + \frac{(aT_s)(bT_s)}{(aT_s) + (bT_s)}\|(u)_N\|_2^2.$$

∎

The *IPESH* similar to the bilinear-transform can be used to synthesize stable digital controllers from continuous-time models. Therefore, we recall the *IPESH*-Transform definition as it applies to SISO *LTI* systems.

Definition 4: [3, Definition 5] Let $H_p(s)$ and $H_p(z)$ denote the respective continuous and discrete time transfer functions which describe a plant. Furthermore, let T_s denote the respective sample and hold time. Finally, denote $\mathcal{Z}\{F(s)\}$ as the z-transform of the sampled time series whose Laplace transform is the expression of $F(s)$, given on the same line in [25, Table 8.1 p.600]. $H_p(z)$ is generated using the following *IPESH*-Transform

$$H_p(z) = \frac{(z-1)^2}{T_s z}\mathcal{Z}\left\{\frac{H_p(s)}{s^2}\right\}.$$

N.B. the term $\frac{z-1}{z}\mathcal{Z}\left\{\frac{H_p(s)}{s^2}\right\}$ represents the exact discrete equivalent for the *LTI* system $\frac{H_p(s)}{s}$ preceded by a *ZOH*
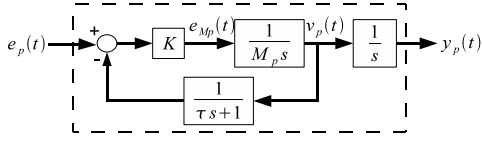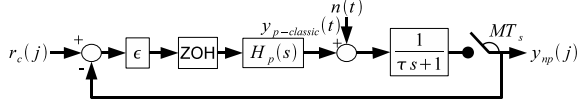
Fig. 5. Plant Dynamics $H_p(s)$

Fig. 6. The classical digital-control-design for position tracking

[25, p. 622] as noted in a detailed proof of [3, Lemma 5] which shows that the *IPESH*-Transform is a scaled version ($k = \frac{1}{T_s}$) of the *IPESH* (Definition 3). The scaling property (Property 1-iv) and Lemma 3 lead directly to Corollary 2.

Corollary 2: If a SISO *LTI* system $H(s)$ is inside the sector $[a,b]$ then $H_p(z)$ resulting from applying the *IPESH*-Transform to $H_p(s)$ is inside the sector $[a,b]$.

III. CONTROLLER VALIDATION & SIMULATION

These results can be readily applied to telemanipulation systems and virtual reality interfaces which use haptic-paddles [11]. Therefore we choose to validate our results through the control of an idealized single-degree-of-freedom haptic paddle. Fig. 5 depicts the idealized *LTI*-model (neglecting gravitational effects) for a single-degree-of-freedom haptic-paddle with mass M_p. The haptic-paddles velocity is controlled with an analog feedback loop in which the control torque is proportional to the feedback gain K. In addition the velocity feedback signal $v_p(t)$ is subject to a low-pass filter with time-constant τ. It can be verified that for $H_p(s) = \frac{Y_p(s)}{E_p(s)}$ if

$$K = \frac{M_p}{\tau}$$ then $H_p(s)$ is inside the sector $[a_p, \infty]$, $a_p = -\tau$.

This nominal plant-system $H_p(s)$ will be controlled using our digital-control network depicted in Fig. 1 in which we shall use a proportional-controller $y_c(j) = k_c e_c(j)$ in which the gain k_c is chosen to satisfy the conditions in Corollary 1 such that

$$-\epsilon^2 a_p = \epsilon^2 \tau < k_c < \frac{1}{\tau} = -\frac{1}{a_p}.$$

In addition K_{MT_s} is chosen so that $r_{ct}(t) = y_p(t)$ at steady-state. The term $r_p(t)$ can be thought of as an over-riding position reference in this framework since force-disturbances are rejected by the velocity feedback loop. If the haptic-paddle hits a wall the resulting steady-state error $(r_c(t) - y_p(t))$ can be applied to an operator proportional to the control gain k_c. Fig. 6 depicts a classic-digital-position-feedback control scheme in which $r_c(j) = y_{p-\text{classic}}(jMT_s)$ at steady-state when $n(t) = 0$.

In order to compare the effects of band-limited noise $n(t)$, the low-pass filtered and noise-corrupted feedback signal $y_{np}(j)$ is periodically sampled every MT_s seconds for the classical-scheme whereas the signal y_p depicted in Fig. 1
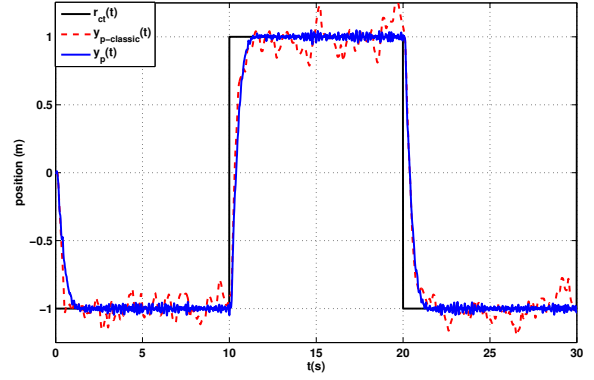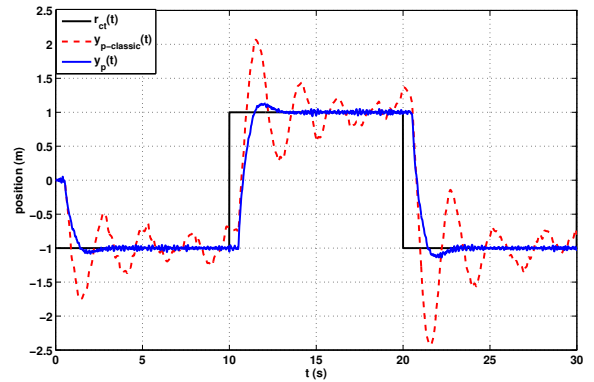

Fig. 7. Baseline tracking response with minimal delay $n(t) \neq 0$.

Fig. 8. Position response with 0.5 second delay.

is corrupted similarly such that $y_p(t) = (H_p e_p(t) + n(t))$. For our high-performance system we filter the noise corrupted signal using the multi-rate-passive-sampler subsystem (Fig. 4) described in Section II-B in which $H_{\text{LPc}}(s) = \frac{1}{\tau s+1}$ (the same analog anti-aliasing low-pass filter used for the classical design). In addition a second-stage digital anti-aliasing filter $H_{LP}(z)$ was synthesized by applying the *IPESH*-Transform to a sixth-order low-pass Butterworth-filter model $H_{LP}(s)$ with passband $\omega_p = \frac{\pi}{MT_s}$ [20, Section 9.7.5].

The simulation parameters are as follows: $\epsilon = 2$, $M_p = 2$ kg, $T_s = .01$ seconds, $M = 10$, $\tau = \frac{MT_s}{\pi}$, $\frac{.4}{\pi} < k_c = 5 < 10\pi$ and $K_{MT_s} = \frac{1}{4}$. Fig. 7 indicates that our high-performance position $y_p(t)$ response tracks the desired reference $r_c(t)$ closer than the classic-digital-control-system response $f_{p-\text{classic}}(t)$ when subject to band-limited noise within the frequency band $[\frac{\pi}{MT_s}, \frac{\pi}{T_s}]$. In addition Fig. 8 indicates that our proposed system is significantly less sensitive to the introduction of a 0.5 second delay between the controller and the plant. In addition, the controller-term $y_{ct}(t)$ in our high-performance-digital control network can provide additional force-feedback to an operator if steady-state error occurs when the haptic-paddle contacts a wall.

IV. CONCLUSIONS

We have provided a set of sufficient conditions to guarantee delay-independent stability for non-passive systems H_p inside the sector $[a_p, b_p]$ $-\infty < a_p < b_p$ for our networked control architecture depicted in Fig. 1. In particular, Theorem 1 and Assumption 1 allow us to derive Theorem 2 which describe the internal network structure depicted in Fig. 3. Lemma 1 shows that a *linear*-passive sampler depicted in Fig. 4 satisfied the key-inequality (12). As a result linear anti-aliasing filters can be introduced which *do not* adversely affect stability or performance. Lemma 2 and Corollary 1 provide the sufficient sector conditions for the controller and plant to achieve the small-gain conditions required of Theorem 3 in order to guarantee L_2^m-stability. Corollary 2 shows that the *IPESH*-Transform can be applied to an analog-controller to synthesize a digital-controller s.t. both controllers are inside the sector $[a, b]$. Simulation results of our proposed architecture applied to *direct position* control of a haptic paddle indicate good performance with low sensitivity to band-limited noise and networked delay.

REFERENCES

[1] P. Antsaklis and J. Baillieul, Eds., *Special Issue: Technology of Networked Control Systems*, ser. Proceedings of the IEEE. IEEE, 2007, vol. 95 number 1.

[2] N. Kottenstette, X. Koutsoukos, J. Hall, J. Sztipanovits, and P. Antsaklis, "Passivity-Based Design of Wireless Networked Control Systems for Robustness to Time-Varying Delays," *Real-Time Systems Symposium, 2008*, pp. 15–24, 2008.

[3] N. Kottenstette, J. Hall, X. Koutsoukos, P. Antsaklis, and J. Sztipanovits, "Digital control of multiple discrete passive plants over networks," *International Journal of Systems, Control and Communications (IJSCC)*, no. Special Issue on Progress in Networked Control Systems, 2009, to Appear.

[4] C. A. Desoer and M. Vidyasagar, *Feedback Systems: Input-Output Properties*. Orlando, FL, USA: Academic Press, Inc., 1975.

[5] G. Niemeyer and J.-J. E. Slotine, "Telemanipulation with time delays," *International Journal of Robotics Research*, vol. 23, no. 9, pp. 873 – 890, 2004.

[6] R. Anderson and M. Spong, "Asymptotic stability for force reflecting teleoperators with time delay," *The International Journal of Robotics Research*, vol. 11, no. 2, pp. 135–149, 1992.

[7] G. Zames, "On the input-output stability of time-varying nonlinear feedback systems. i. conditions derived using concepts of loop gain, conicity and positivity," *IEEE Transactions on Automatic Control*, vol. AC-11, no. 2, pp. 228 – 238, 1966.

[8] J. Willems, *Feedback systems. The analysis of.* London, UK: MIT Press, 1971.

[9] N. Kottenstette and J. Porter, "Digital passive attitude and altitude control schemes for quadrotor aircraft," Institute for Software Integrated Systems, Vanderbilt University, Nashville, TN, Report, 11/2008 2008, to Appear ICCA09. [Online]. Available: http://www.isis.vanderbilt.edu/node/4051

[10] N. Kottenstette and N. Chopra, "Lm2-stable digital-control networks for multiple continuous passive plants," *1st IFAC Workshop on Estimation and Control of Networked Systems (NecSys'09)*, 2009.

[11] S. Hirche and M. Buss, "Transparent Data Reduction in Networked Telepresence and Teleaction Systems. Part II: Time-Delayed Communication," *Presence: Teleoperators and Virtual Environments*, vol. 16, no. 5, pp. 532–542, 2007.

[12] N. Chopra, P. Berestesky, and M. Spong, "Bilateral teleoperation over unreliable communication networks," *IEEE Transactions on Control Systems Technology*, vol. 16, no. 2, pp. 304–313, 2008.

[13] S. Hirche, T. Matiakis, and M. Buss, "A distributed controller approach for delay-independent stability of networked control systems," *Automatica*, vol. 45, no. 8, pp. 1828–1836, 2009.

[14] D. J. Hill, "Dissipative nonlinear systems: Basic properties and stability analysis," *Proceedings of the 31$^{\text{st}}$ IEEE Conference on Decision and Control*, pp. 3259–3264, 1992.
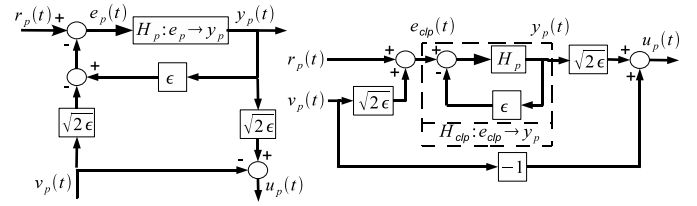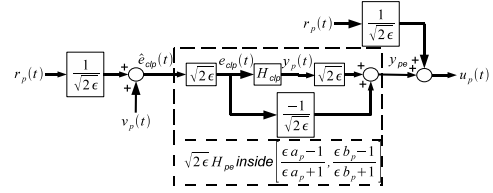
[15] D. J. Hill and P. J. Moylan, "The stability of nonlinear dissipative systems," *IEEE Transactions on Automatic Control*, vol. AC-21, no. 5, pp. 708 – 11, 1976.

[16] ——, "Stability results for nonlinear feedback systems," *Automatica*, vol. 13, pp. 377–382, 1977.

[17] G. C. Goodwin and K. S. Sin, *Adaptive Filtering Prediction and Control*. Englewood Cliffs, New Jersey 07632: Prentice-Hall, Inc., 1984.

[18] W. M. Haddad and V. S. Chellaboina, *Nonlinear Dynamical Systems and Control: A Lyapunov-Based Approach*. Princeton, New Jersey, USA: Princeton University Press, 2008.

[19] R. J. Anderson and M. W. Spong, "Bilateral control of teleoperators with time delay," *Proceedings of the IEEE Conference on Decision and Control Including The Symposium on Adaptive Processes*, pp. 167 – 173, 1988.

[20] A. Oppenheim, A. Willsky, and S. Nawab, *Signals and systems*. Prentice hall Upper Saddle River, NJ, 1997.

[21] N. Kottenstette and P. Antsaklis, "Wireless Control of Passive Systems Subject to Actuator Constraints," *47th IEEE Conference on Decision and Control, 2008. CDC 2008*, pp. 2979–2984, 2008.

[22] S. Stramigioli, C. Secchi, A. J. van der Schaft, and C. Fantuzzi, "Sampled data systems passivity and discrete port-hamiltonian systems," *IEEE Transactions on Robotics*, vol. 21, no. 4, pp. 574 – 587, 2005.

[23] J.-H. Ryu, Y. S. Kim, and B. Hannaford, "Sampled- and continuous-time passivity and stability of virtual environments," *IEEE Transactions on Robotics*, vol. 20, no. 4, pp. 772 – 6, 2004.

[24] N. Kottenstette and P. Antsaklis, "Stable digital control networks for continuous passive plants subject to delays and data dropouts," *46th IEEE Conference on Decision and Control*, pp. 4433–4440, 2007.

[25] G. F. Franklin, J. D. Powell, and A. Emami-Naeini, *Feedback Control of Dynamic Systems*, 5th ed. Prentice-Hall, 2006.

Fig. 9. Plant-r_p-v_p-y_p-u_p-network realization and initial transformation.

Fig. 10. Final Plant-r_p-v_p-y_p-u_p-network realization.

APPENDIX

Fig. 9 depicts a graphical realization of (7) on the left-hand-side (LHS), and the first obvious graphical-transformation on the right-hand-side (RHS) in which we denote closed-loop-transformation of the plant H_p in terms of the feedback-gain ϵ as $H_{\mathsf{clp}} : e_{\mathsf{clp}} \to y_p$ in which

$$e_{\mathsf{clp}}(t) = r_p(t) + \sqrt{2\epsilon}v_p(t) = e_p(t) + \epsilon y_p(t). \qquad (29)$$

In order to simplify discussion and to leverage Theorem 1 we use Assumption 1 in order to state the following corollary:

Corollary 3: If Assumption 1 is satisfied then $H_{\mathsf{clp}} : e_{\mathsf{clp}} \to y_p$ is inside the sector $\left[\frac{a_p}{1+\epsilon a_p}, \frac{b_p}{1+\epsilon b_p} \right]$.
Next we transform the RHS realization in Fig. 9 to the final form depicted in Fig. 10.
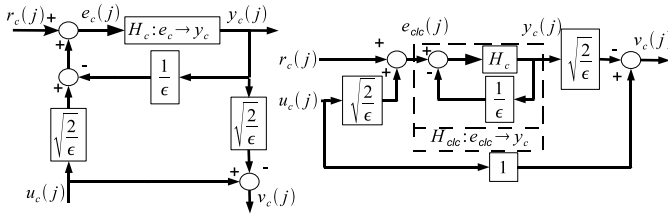
Fig. 11. Controller-r_c-u_c-e_p-v_c-network realization and initial transformation.

Fig. 12. Final Controller-r_c-u_c-y_c-v_c-network realization.

Lemma 4: The RHS of Fig. 9 can be transformed to the final form depicted in Fig. 10 (in which $H_{\mathsf{pe}}e_{\mathsf{clp}} = \sqrt{2\epsilon}H_{\mathsf{clp}}e_{\mathsf{clp}} - \frac{1}{\sqrt{2\epsilon}}e_{\mathsf{clp}}$). In addition if Assumption 1 is satisfied, then
$\sqrt{2\epsilon}H_{\mathsf{pe}}\hat{e}_{\mathsf{clp}}(t)$ is inside the sector $\left[\frac{\epsilon a_p - 1}{\epsilon a_p + 1}, \frac{\epsilon b_p - 1}{\epsilon b_p + 1}\right]$.

Proof: From Fig. 10 it is clear that,

$$e_{\mathsf{clp}}(t) = \sqrt{2\epsilon}\left(\frac{1}{\sqrt{2\epsilon}}r_p(t) + v_p(t)\right) = r_p(t) + \sqrt{2\epsilon}v_p(t)$$

which satisfies (29), next from Fig. 10 it is clear that,

$$
\begin{aligned}
u_p(t) &= \sqrt{2\epsilon}y_p(t) - \frac{1}{\sqrt{2\epsilon}}e_{\mathsf{clp}}(t) + \frac{1}{\sqrt{2\epsilon}}r_p(t) \\
&= \sqrt{2\epsilon}y_p(t) - \frac{1}{\sqrt{2\epsilon}}\left(r_p(t) + \sqrt{2\epsilon}v_p(t)\right) + \frac{1}{\sqrt{2\epsilon}}r_p(t) \\
&= \sqrt{2\epsilon}y_p(t) - v_p(t).
\end{aligned}
$$

which satisfies (7) in regards to $u_p(t)$. From Corollary 3 we have that $H_{\mathsf{clp}} : e_{\mathsf{clp}} \to y_p$ is inside the sector $\left[\frac{a_p}{1+\epsilon a_p}, \frac{b_p}{1+\epsilon b_p}\right]$. From the scaling property (Property 1-iv), we have that $H_{\mathsf{clp}}\sqrt{2\epsilon} = \sqrt{2\epsilon}H_{\mathsf{clp}}$ in which $\sqrt{2\epsilon}H_{\mathsf{clp}}$ is inside the sector $\left[\sqrt{2\epsilon}\frac{a_p}{1+\epsilon a_p}, \sqrt{2\epsilon}\frac{b_p}{1+\epsilon b_p}\right]$. Using the sum-rule (Property 1-v) we have that

$$H_{\mathsf{pe}} \text{ is inside the sector}$$
$$\left[\frac{-1}{\sqrt{2\epsilon}} + \sqrt{2\epsilon}\frac{a_p}{1+\epsilon a_p}, \frac{-1}{\sqrt{2\epsilon}} + \sqrt{2\epsilon}\frac{b_p}{1+\epsilon b_p}\right]$$
$$\text{solving for } a_{\mathsf{pe}} \text{ we have}$$
$$a_{\mathsf{pe}} = \frac{-1}{\sqrt{2\epsilon}} + \sqrt{2\epsilon}\frac{a_p}{1+\epsilon a_p} = \frac{1}{\sqrt{2\epsilon}}\left(\frac{2\epsilon a_p - \epsilon a_p - 1}{\epsilon a_p + 1}\right)$$
$$\text{therefore } H_{\mathsf{pe}} \text{ is inside the sector}$$
$$\left[\frac{1}{\sqrt{2\epsilon}}\left(\frac{\epsilon a_p - 1}{\epsilon a_p + 1}\right), \frac{1}{\sqrt{2\epsilon}}\left(\frac{\epsilon b_p - 1}{\epsilon b_p + 1}\right)\right]$$
$$\text{finally from the scaling property we have that}$$
$$\sqrt{2\epsilon}H_{\mathsf{pe}} \text{ is inside the sector } \left[\frac{\epsilon a_p - 1}{\epsilon a_p + 1}, \frac{\epsilon b_p - 1}{\epsilon b_p + 1}\right].$$

∎

Fig. 11 depicts a graphical realization of (8) on the left-hand-side (LHS), and the first obvious graphical-transformation on the right-hand-side (RHS) in which we denote closed-loop-transformation of the controller H_c in terms of the feedback-gain $\frac{1}{\epsilon}$ as $H_{\mathsf{clc}} : e_{\mathsf{clc}} \to y_c$ in which

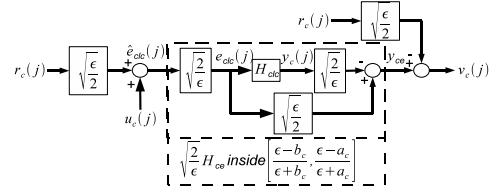$$e_{\mathsf{clc}}(j) = r_c(j) + \sqrt{\frac{2}{\epsilon}}u_c(j) = e_c(j) + \frac{1}{\epsilon}y_c(j). \quad (30)$$

Which allows us to state the following corollary:

Corollary 4: If Assumption 1 is satisfied then $H_{\mathsf{clc}} : e_{\mathsf{clc}} \to y_c$ is inside the sector $\left[\frac{\epsilon a_c}{\epsilon + a_c}, \frac{\epsilon b_c}{\epsilon + b_c}\right]$.

Next we transform the RHS realization in Fig. 11 to the final form depicted in Fig. 12.

Lemma 5: The RHS of Fig. 11 can be transformed to the final form depicted in Fig. 12 (in which $H_{\mathsf{ce}}e_{\mathsf{clc}} = -\sqrt{\frac{2}{\epsilon}}H_{\mathsf{clc}}e_{\mathsf{clc}} + \sqrt{\frac{\epsilon}{2}}e_{\mathsf{clc}}$). In addition if Assumption 1 is satisfied, then

$$\sqrt{\frac{2}{\epsilon}}H_{\mathsf{ce}}\hat{e}_{\mathsf{clc}}(j) \text{ is inside the sector } \left[\frac{\epsilon - b_c}{\epsilon + b_c}, \frac{\epsilon - a_c}{\epsilon + a_c}\right].$$

Proof: From Fig. 12 it is clear that,

$$e_{\mathsf{clc}}(j) = \sqrt{\frac{2}{\epsilon}}\left(\sqrt{\frac{\epsilon}{2}}r_c(j) + u_c(j)\right) = r_c(j) + \sqrt{\frac{2}{\epsilon}}u_c(j)$$

which satisfies (30), next from Fig. 12 it is clear that,

$$
\begin{aligned}
v_c(j) &= -\sqrt{\frac{2}{\epsilon}}y_c(j) + \sqrt{\frac{\epsilon}{2}}e_{\mathsf{clc}}(j) - \sqrt{\frac{\epsilon}{2}}r_c(j) \\
&= -\sqrt{\frac{2}{\epsilon}}y_c(j) + \sqrt{\frac{\epsilon}{2}}\left(r_c(j) + \sqrt{\frac{2}{\epsilon}}u_c(j)\right) - \sqrt{\frac{\epsilon}{2}}r_c(j) \\
&= -\sqrt{\frac{2}{\epsilon}}y_c(j) + u_c(j).
\end{aligned}
$$

which satisfies (8) in regards to $v_c(j)$. From Corollary 4 we have that $H_{\mathsf{clc}} : e_{\mathsf{clc}} \to y_c$ is inside the sector $\left[\frac{\epsilon a_c}{\epsilon + a_c}, \frac{\epsilon b_c}{\epsilon + b_c}\right]$. From the scaling property, we have that $-H_{\mathsf{clc}}\sqrt{\frac{2}{\epsilon}} = -\sqrt{\frac{2}{\epsilon}}H_{\mathsf{clc}}$ in which $-\sqrt{\frac{2}{\epsilon}}H_{\mathsf{clc}}$ is inside the sector $\left[-\sqrt{\frac{2}{\epsilon}}\frac{\epsilon b_c}{\epsilon + b_c}, -\sqrt{\frac{2}{\epsilon}}\frac{\epsilon a_c}{\epsilon + a_c}\right]$. Using the sum-rule we have that

$$H_{\mathsf{ce}} \text{ is inside the sector}$$
$$\left[\sqrt{\frac{\epsilon}{2}} - \sqrt{\frac{2}{\epsilon}}\frac{\epsilon b_c}{\epsilon + b_c}, \sqrt{\frac{\epsilon}{2}} - \sqrt{\frac{2}{\epsilon}}\frac{\epsilon a_c}{\epsilon + a_c}\right]$$
$$\text{solving for } b_{\mathsf{ce}} \text{ we have}$$
$$b_{\mathsf{ce}} = \sqrt{\frac{\epsilon}{2}} - \sqrt{\frac{2}{\epsilon}}\frac{\epsilon a_c}{\epsilon + a_c} = \sqrt{\frac{\epsilon}{2}}\left(1 - \frac{2a_c}{\epsilon + a_c}\right)$$
$$\text{therefore } H_{\mathsf{ce}} \text{ is inside the sector}$$
$$\left[\sqrt{\frac{\epsilon}{2}}\left(\frac{\epsilon - b_c}{\epsilon + b_c}\right), \sqrt{\frac{\epsilon}{2}}\left(\frac{\epsilon - a_c}{\epsilon + a_c}\right)\right]$$
$$\text{finally from the scaling property we have that}$$
$$\sqrt{\frac{2}{\epsilon}}H_{\mathsf{ce}} \text{ is inside the sector } \left[\frac{\epsilon - b_c}{\epsilon + b_c}, \frac{\epsilon - a_c}{\epsilon + a_c}\right].$$

∎